Available online at www.sciencedirect.com

ScienceDirect

Ceramics International 40 (2014) 1045–1049

CERAMICS INTERNATIONAL

www.elsevier.com/locate/ceramint

Transmission electron microscopy study on crack propagation characteristics of pressureless sintered 15R-β-U Sialon-polytypoid composite

Zhaohui Huang[a], Saifang Huang[a,b], Minghao Fang[a,*], Yan-gai Liu[a], Xin Ouyang[a,b], Juntong Huang[a]

[a]School of Materials Science and Technology, China University of Geosciences (Beijing), Beijing 100083, PR China
[b]Department of Chemical & Materials Engineering, The University of Auckland, Private Bag 92019, New Zealand

Received 22 June 2013; accepted 27 June 2013
Available online 3 July 2013

Abstract

Fabrication of densified 15R-β-U Sialon-polytypoid composite has been reported previously using a pressureless sintering (PLS) method at a relatively low temperature (1650 °C). The mechanical properties of this material are as good as those high temperature heat-pressed Sialon-polytypoids. In this study, the crack propagation characteristics were investigated to interpret the fracture behaviors of this material by transmission electron microscopy (TEM) technique. A schematic diagram was proposed according to the experimental results. The composite mainly fractures via a transgranular mode as indicated by the propagation routes of cracks. Subcrack branches can be induced by deflecting or shifting of cracks intergranularly or within a grain. The bonding strength of interface within grains is higher than the bonding force within the layer structure of 15R, contributing to the excellent mechanical properties of the pressureless sintered composite.

Keywords: B. Electron microscopy; B. Composites; C. Fracture; D. Sialon

1. Introduction

There is an enormous family of Sialon phases in the five-component *Ln*–Si–Al–O–N systems [1–3], such as α- [4], B- [5], J- [6], M- [7], N- [8], S- [9], W- [10], U- [11] and JEM- [12] phases. A variety of Sialon materials [13–15] with desirable properties can be fabricated in these systems via compositional design. Their achievable sintering characteristics and excellent mechanical/thermal properties make these materials suitable for a variety of applications, such as gas-turbine engines, milling medium, metal-forming tools, and metal-cutting tools and wear-resistant ceramic components [2,16]. In comparison with other Sialon phases, AlN-polytypoids possess unique properties of that their elevated temperature mechanical properties are better than the room-temperature properties [13,17–19], which is probably related to the laminar structure of polytypoids. Therefore, AlN-polytypoids are promising and have good performance as high temperature structural materials.

AlN-polytypoid phases are considered to possess needle or elongated platelet morphology, which would have a strengthening and toughening effect on themselves *in situ* or on the matrix phases. Wang et al. [19] have investigated the effect of additives on the sintering of AlN-polytypoids, especially 15R [20]. In the past years, the reported AlN-polytypoids ceramics were normally densified using a relevant complex technology, i.e. hot-pressing at temperatures higher than 1750 °C [17–19]. In our recent study [13], we have reported the densified Sialon-polytypoid composite fabricated by compositional design via transient liquid-phase pressureless sintering at relatively low temperature (1650 °C). The sintered composite had excellent mechanical properties and was mainly composed of 15R polytypoid ($SiAl_4O_2N_4$), β-Sialon ($Si_3Al_3O_3N_5$), and U-phase Sialon ($Gd_3Si_{2.5}Al_{3.5}O_{11.5}N_{0.5}$), thereby denoting the material as 15R-β-U Sialon-polytypoid composite. The flexural strength, fracture toughness and Vickers hardness of the composite were about 340 MPa, 3.44 MPa $m^{1/2}$ (single-edge

*Corresponding author. Tel./fax: +86 10 82322186.
E-mail address: fmh@cugb.edu.cn (M. Fang).

0272-8842/$ - see front matter © 2013 Elsevier Ltd and Techna Group S.r.l. All rights reserved.
http://dx.doi.org/10.1016/j.ceramint.2013.06.102

notched beam (SENB) method) and 11.72 GPa, respectively [13].

Although we found that the Sialon-polytypoid composite demonstrates both intercrystalline and transcrystalline fracture modes in the previous work [13], it is still unclear on how the different Sialon phases behave when a fracture takes place in this type of Sialon composite. The goal of this study is to investigate the fracture behavior of this composite using TEM technique. The fashions of crack propagation were revealed to illustrate how cracks come across with 15R, β-Sialon and U-phase Sialon grains.

2. Experimental procedure

15R-β-U Sialon-polytypoid composite was prepared using the optimal sintering additive Gd_2O_3 for investigating the crack behavior of the material. The optimization process of sintering additive was reported elsewhere [13]. The composition of the sample was designed as Gd_2O_3 9.17 wt%, Si_3N_4 35.47 wt%, AlN 37.31 wt%, and Al_2O_3 18.05 wt%. The starting powder was mixed for 12 h by ball milling in water-free ethanol with an agate media, and then dried at 70 °C for 12 h. Subsequently, the powders were molded to be bar samples with dimensions of 3 mm × 4 mm × 30 mm by uniaxial pressing at 30 MPa in a steel die, and then pressed at 200 MPa by cold isostatic pressing. The samples were placed in graphite crucibles and packed in a protective BN powder bed. Finally, the pressureless sintering of bar samples was conducted in a high-temperature furnace backfilled with 1 atm nitrogen gas, by heating at a ramp rate of 5 °C min^{-1} from room temperature to 1650 °C and then holding for 4 h at this temperature. After pressureless sintering of the samples, 15R, β-Sialon and U-phase Sialon formed in situ and dispersed evenly in the material. .

High-resolution transmission electron microscopy (HREM) and selected area electron diffraction (SAED) investigations were carried out using transmission electron microscopy (TEM) (JEOL JEM-2100, Tokyo, Japan, accelerating voltage 200 keV, 2.7k × 4k Gatan CCD camera, Gatan Inc., Pleasanton, CA) with Oxford INCA (Oxfordshire, UK) energy-

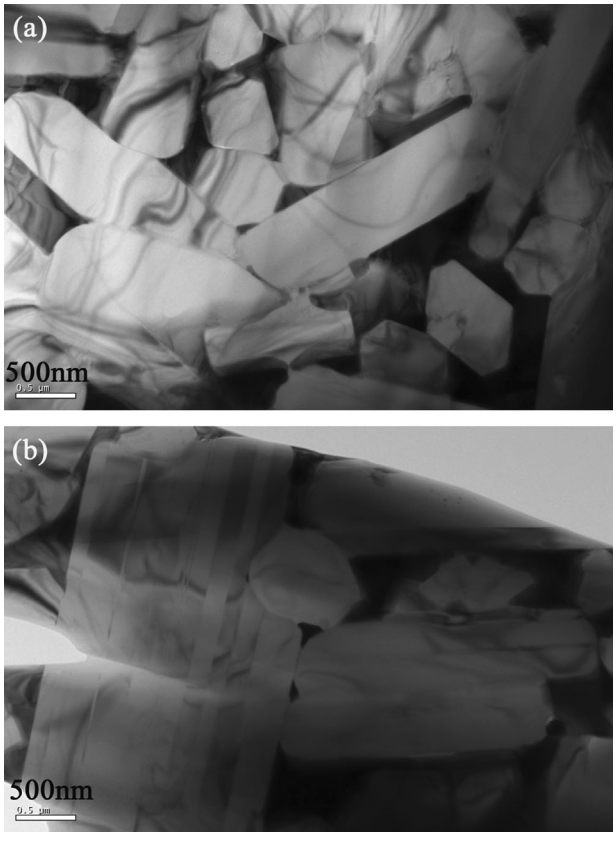

Fig. 1. Mosaic structure of β-Sialon in three 15R grains observed in the Sialon-polytypoid composite, where β-Sialon grain was embedded into a twinned 15R grain.

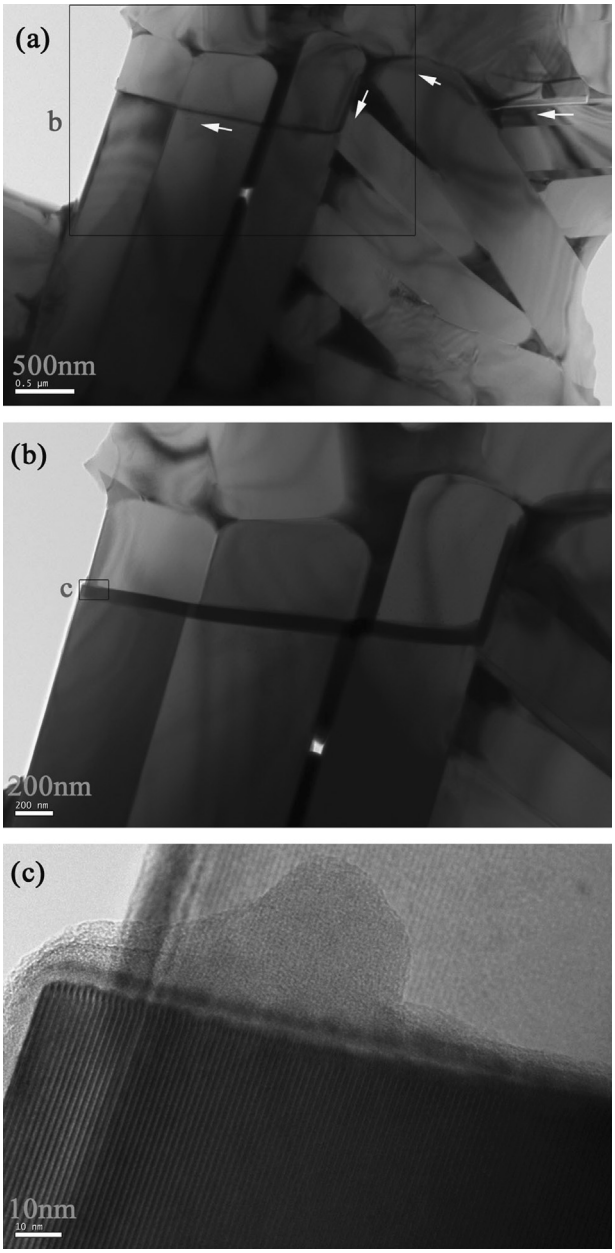

Fig. 2. TEM images of a crack in the composite. (a) The path of crack in the material, (b) the enlarged TEM image of crack across three 15R grains, and (c) the high-resolution TEM image of crack in the magnified area marked with "c" in Fig. 2b.

dispersive spectrometer (EDS) for microprobe elemental analysis. Standard methods and carbon coating were applied for preparation of thin foils for the TEM observation. The cracks were self-introduced into the foils during the preparation process without breaking the foils.

3. Results and discussion

Systematic investigation on the effect of additive, the microstructure and properties of Gd-doped composite was previously reported [13]. Some TEM results of crystalline phases in the material and crack propagation were also shown in that paper. The intergranular U-phase Gd-Sialon implies a transient liquid phase sintering mechanism of the densification process of this material [13]. In the present work, we did further investigation on the microstructure and crack behavior of the Sialon-polytypoid composite via high-resolution TEM observation.

TEM image in Fig. 1a shows the typical microstructure of the composite with platelet grains, the hexagonal grains and the dark intergranular areas. They were identified by energy-dispersive X-ray spectroscopy (EDS) analysis to be 15R, β-Sialon and U-phase Gd-Sialon, respectively. Fig. 1b presents the mosaic structure of β-Sialon in three 15R grains observed in the Sialon-polytypoid composite. The mosaic structure was also found in β-Sialon-12H ceramics composites reported by Wang et al. [21]. The twin structure of 15R was identified in Fig. 1b as well. The β-Sialon grain was embedded into the twinned 15R grain without changing the structure of twin boundaries. It implies that the twin structure of 15R grain was probably formed due to the stress raised from the growth of the embedded β-Sialon grain.

Fig. 2a shows a crack propagating in the material with intercrystalline fracture and transcrystalline fracture. An image of transcrystalline fracture in 15R grains with higher

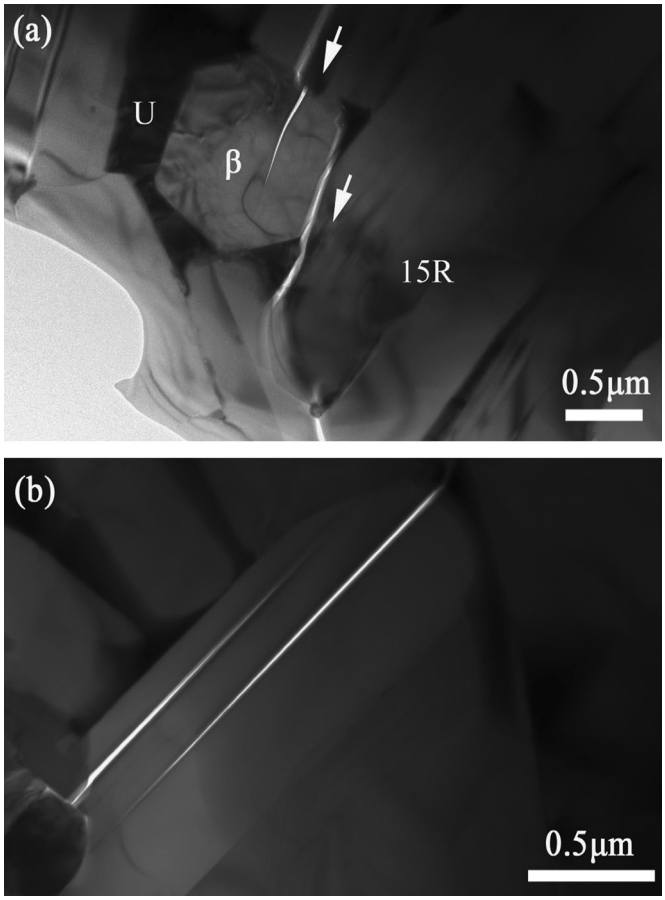

Fig. 3. Atomically sharp cracks in (a) β-Sialon and (b) 15R grains.

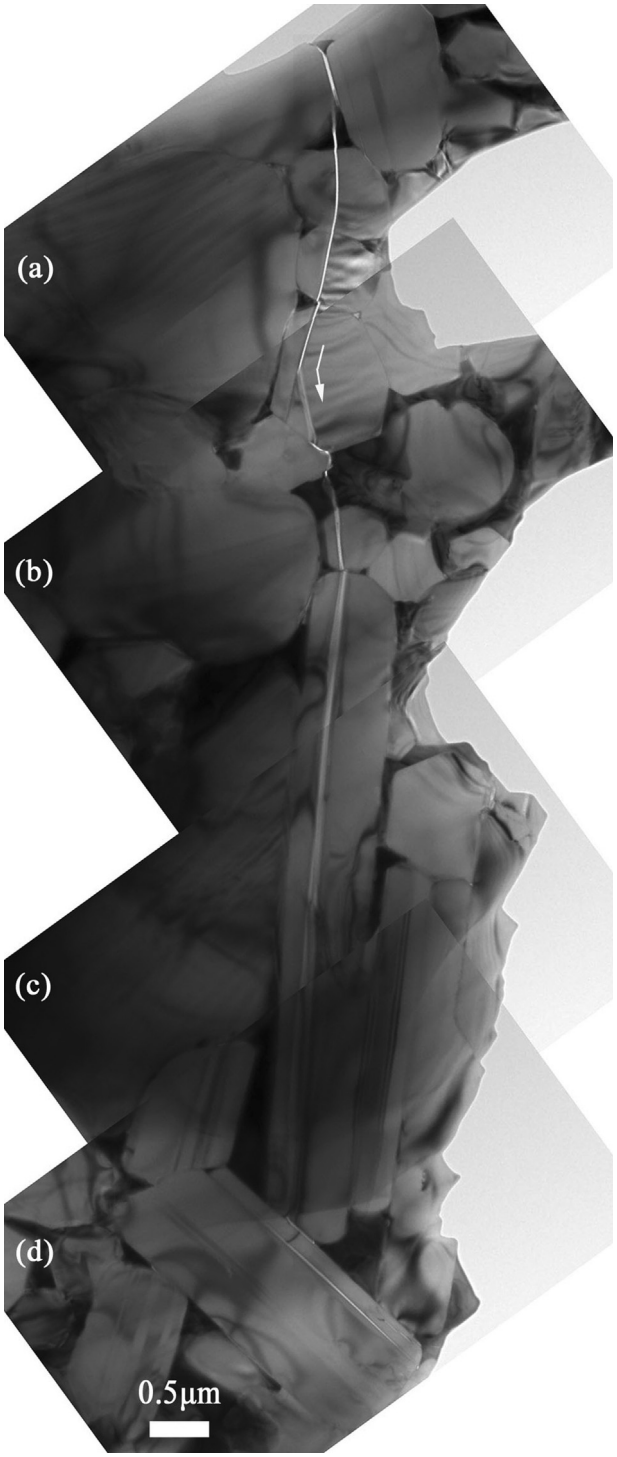

Fig. 4. Crack propagation in the Sialon-polytypoid composite.

magnification is shown in Fig. 2b. The 15R grains were separated into two parts with a shift of about 20 nm. A very thin amorphous film resulting from the fracture was observed at the edge of fractured grain boundary, as clearly shown in Fig. 2c. The lattice of 15R apparently displayed on both sides of the fractured grain.

In addition, some cracks were found to stop in the 15R and β-Sialon grains but triggered another cracks. The intergranular shift of crack was observed in β-Sialon grain (Fig. 3a) and the shift was also found in 15R polytypoid grain (Fig. 3b). The former mode presented when the crack come across and ended in β-Sialon grain, which may be attributed to that the bonding force in atomic level of [(Si,Al)(O,N)4] tetrahedral is relatively strong. On the other hand, the later mode occurred when the crack went through 15R grain. The laminar structure of 15R, like other polytypoids phase do, may easily accumulate the stress, which results from the initial crack of the 15R grain, in other layers. This mode indicates that the bonding strength of interface surrounding this grain may be higher than the bonding force in the layer structure of 15R. The atomically sharp cracks in this composite were similar with those reported in 15R AlN-polytypoid materials by Tanaka et al. [22], which opened between two adjacent layers in the crystal. As suggested in their work, the lattice deformation of 15R around the crack tips could be predicted from the linear fracture mechanics model.

Particularly, a long crack was observed by TEM in the material, as shown in Fig. 4. The crack initiated intergranularly at the top of the figure, then went through the material and finally ended up in a 15R grain at the bottom. The transgranular cracks took place in most of grains along the propagation route. It is interesting to see that the crack ended in a 15R grain by shifting from an intergranular crack between two 15R grains to a transgranular crack in 15R grain where the crack was stopped. As can be seen in the second image from the top of Fig. 4, a crack deflection (guided by an arrow) can be seen in the β-Sialon grain with an angle of ~150°. It indicates that there was a defect located in the β-Sialon grain, and the deflection direction may be ascribed to the hexagonal structure of β-Sialon phase. Therefore, when defects/stress present at a certain area, they may induce the deflection of crack along the weak crystal plane.

Fig. 5a shows nano-crack branches originated from a single crack in 15R-β-U Sialon-polytypoid composite. The one with bigger cracks on the left-hand side transgranularly propagated through 15R grains, and the other branch shifted intergranularly along the interface of 15R and β-Sialon grains and then broke the β-Sialon grain. Fig. 5b shows the higher magnification of the critical place where the crack entered into the 15R grain. In order to tell how the crack affect the structure in atomic level, the high-resolution TEM images of the cracks in Fig. 5b, as indicated, are shown in Fig. 5c–d. Two cracks as indicated by "1" and "2" in the Fig. 5b are obviously

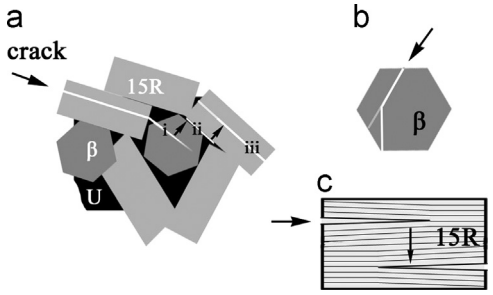

Fig. 6. Schematic illustration of crack deflection and shifting in the Sialon-polytypoid composite. (a) Subcrack induced by shifting intergranularly i.e. from crack "i" to subcrack "ii" (Fig. 3a), and from subcrack "ii" to subcrack "iii" (Fig. 4a); (b) crack deflecting transgranularly (Fig. 4d) and (c) crack shifting within a grain (Fig. 3b).

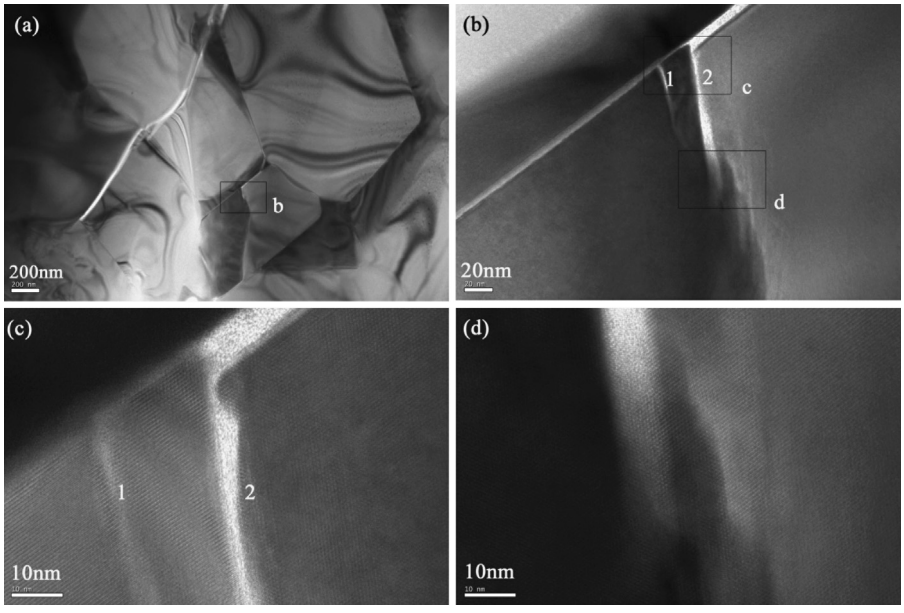

Fig. 5. TEM image of nano cracks in 15 R-β-U Sialon composite. (a) The crack branches through the composite, (b) the magnified image of area marked with "b" in Fig. 5a, (c) and (d) the HREM image of areas marked with "c" and "d" in Fig. 5b.

presented, and the high-resolution image in Fig. 5c illustrates that the two parts separated by crack "1" were just slightly shifted whereas the crack "2" moved downward the grain on the right-hand side. The fractured edge was not straight. It is suggested from Fig. 5d that the lattice fringes of β-Sialon are distorted by the crack. It is likely that more energy will be dissipated for a twisted route than a straight crack.

The schematic illustration of crack deflection and shifting in the Sialon-polytypoid composite is presented in Fig. 6. As illustrated in Fig. 6a, subcrack "ii" is induced from crack "i" by shifting intergranularly (with respect to Fig. 3a), and it can induce subcrack "iii" via the same mode (as can be seen in Fig. 4a). Fig. 6b shows the mode that crack deflects transgranularly in a β-Sialon grain (corresponding to Fig. 4d), while Fig. 6c demonstrates the mode that crack shifts transgranularly within a 15R grain (see Fig. 3b).

4. Conclusions

Fracture characteristics of 15R-β-U Sialon-polytypoid composite were investigated by observation of propagation route in the material with the aid of TEM. A typical mosaic structure was observed in the Sialon-polytypoid composite in this study, which was similar to that in β-Sialon-12H ceramics reported by Wang et al. The cracks in β-Sialon grains caused slight deformation of the lattice. When a micro-crack meets 15R grains, it is more likely to have a transgranular propagation, and could induce crack branches by deflecting or shifting. Accordingly, the bonding strength of the interface in the composite is probably higher than the bonding force in the layer structure of 15R crystal, giving rise to the excellent mechanical properties of the pressureless sintered Sialon-polytypoid composite as previously reported.

Acknowledgments

This work was financially supported by National Natural Science Foundation of China (NSFC Grant nos. 51032007 and 50972134), New Star Technology Plan of Beijing (Grant no. 2007A080), the Fundamental Research Funds for the Central Universities (Grant no. 2011PY0173) and the Innovation and Technology Fund for Postgraduate of China University of Geosciences (Beijing). S.F. Huang and X. Ouyang would like to thank the China Scholarship Council (CSC) for providing a Doctoral Scholarship for their Ph.D. study in The University of Auckland.

References

[1] S.F. Huang, Z.H. Huang, M.H. Fang, Y.G. Liu, J.T. Huang, J.Z. Yang, Nd-Sialon microcrystals with an orthogonal array, Crystal Growth and Design 10 (6) (2010) 2439–2442.

[2] V.A. Izhevskiy, L.A. Genova, J.C. Bressiani, F. Aldinger, Progress in SiAlON ceramics, Journal of the European Ceramic Society 20 (13) (2000) 2275–2295.

[3] J. Huang, H. Zhou, Z. Huang, G. Liu, M. Fang, Y.G. Liu, Preparation and formation mechanism of elongated (Ca,Dy)-alpha-Sialon powder via carbothermal reduction and nitridation, Journal of the American Ceramic Society 95 (6) (2012) 1871–1877.

[4] S. Hampshire, H.K. Park, D.P. Thompson, K.H. Jack, Alpha'-Sialon ceramics, Nature 274 (5674) (1978) 880–882.

[5] M.F. Gonon, J.C. Descamps, F. Cambier, D.P. Thompson, Determination and refinement of the crystal structure of M_2SiAlO_5N "B-phase" (M=Y, Er, Yb), Ceramics International 26 (1) (2000) 105–111.

[6] J. Takahashi, H. Yamane, N. Hirosaki, Y. Yamamoto, M. Mitomo, M. Shimada, Crystal structure of rare-earth silicon-oxynitride J-phases, $Ln_4Si_2O_7N_2$, Journal of the European Ceramic Society 25 (6) (2005) 793–799.

[7] Y.B. Cheng, D.P. Thompson, Aluminum-containing nitrogen melilite phases, Journal of the American Ceramic Society 77 (1) (1994) 143–148.

[8] J. Grins, Z.J. Shen, S. Esmaeilzadeh, P. Berastegui, The structures of the Ce and La N-phases $RE_3Si_{8-x}Al_xN_{11-x}O_{4+x}$ ($x\approx1.75$ for RE=Ce, $x\approx1.5$ for RE=La), determined by single-crystal X-ray and time-of-flight neutron powder diffraction, respectively, Journal of Materials Chemistry 11 (9) (2001) 2358–2362.

[9] Z.J. Shen, J. Grins, S. Esmaeilzadeh, H. Ehrenberg, Preparation and crystal structure of a new Sr containing sialon phase $Sr_2Al_{x-}Si_{12-x}N_{16-x}O_{2+x}$ ($x\approx2$), Journal of Materials Chemistry 9 (4) (1999) 1019–1022.

[10] D.P. Thompson, New grain-boundary phases for nitrogen ceramics, in: Proceeding of the Materials Research Society Fall Meeting, December 1, 1992–December 3, 1992, vol. 287, Materials Research Society, Boston, MA, USA, 1993, pp. 79–92.

[11] C.J. Spacie, K. Liddell, D.P. Thompson, The U-phase in heat-treated Sialon ceramics, Journal of Materials Science Letters 7 (2) (1988) 95–96.

[12] S.F. Huang, Z.H. Huang, Y.G. Liu, M.H. Fang, Crystal structure of $NdSi_{6-z}Al_{1+z}O_zN_{10-z}$ ($z=0.4$) determined by single-crystal X-ray diffraction, Dalton Transactions 40 (6) (2011) 1261–1266.

[13] S. Huang, Z. Huang, Y.g. Liu, M. Fang, L. Yin, J. Huang, Microstructural and mechanical characterization of pressure-less sintered AlN-polytypoid based composites by compositional design, Journal of the American Ceramic Society 95 (6) (2012) 2044–2050.

[14] Z.H. Huang, J.Z. Yang, Y.G. Liu, M.H. Fang, J.T. Huang, H.R. Sun, S. F. Huang, Novel Sialon-based ceramics toughened by ferro-molybdenum alloy, Journal of the American Ceramic Society 95 (3) (2012) 859–861.

[15] M.J. Pomeroy, E. Nestor, R. Ramesh, S. Hampshire, Properties and crystallization of rare-earth Si–Al–O–N glasses containing mixed trivalent modifiers, Journal of the American Ceramic Society 88 (4) (2005) 875–881.

[16] J.Z. Yang, Z.H. Huang, X.Z. Hu, M.H. Fang, Y.G. Liu, J.T. Huang, Microstructure characteristics of FeMo-Sialon ceramic composite, Materials Science and Engineering A 528 (4–5) (2011) 2196–2199.

[17] K. Komeka, A. Tsuge, Formation of AlN polytype ceramics and some of their properties, Journal of the Ceramic Society of Japan 89 (1981) 615–620.

[18] H.X. Li, W.Y. Sun, D.S. Yan, Mechanical properties of hot-pressed 12H ceramics, Journal of the European Ceramic Society 15 (7) (1995) 697–701.

[19] P.L. Wang, W.Y. Sun, D.S. Yan, Mechanical properties of AlN-polytypoids—15R, 12H and 21R, Materials Science and Engineering A 272 (2) (1999) 351–356.

[20] P.L. Wang, Y.X. Jia, W.Y. Sun, Fabrication of 15R AlN-polytypoid ceramics, Materials Letters 41 (1999) 78–82 Compendex.

[21] H. Wang, W.Y. Sun, H.R. Zhuang, J.W. Feng, T.S. Yen, Microstructural observation of beta'-Sialon-12H multiphase ceramics by HREM, Materials Letters 17 (3-4) (1993) 131–136.

[22] H. Tanaka, Y. Bando, Y. Inomata, M. Mitomo, Atomically sharp crack in 15R-Sialon, Journal of the American Ceramic Society 71 (1) (1988) C32–C33.